Scientific Journal of Riga Technical University
Power and Electrical Engineering
DOI: 10.2478/v10144-011-0021-y 2011
Volume 29

Preliminary Circuit Design for Robotics Environment Mapping Utilizing Ambient Light, Reflected Light and Stationary Infrared Radiation

Leslie R. Adrian, *Riga Technical University*

Abstract **– The paper deals with robotics mobility and a proposed topology for the acquisition of the necessary data to enable accurate mapping of a given environment, be that for basic maneuverability, (obstacle avoidance) or for higher level applications such as fire detection or item location. The topology is composed of a four layered system of analogue components which lends itself not only to excellent linearity but allows the system to control peripheral devices directly through any logic configuration, or to provide data needed for microcontrollers and their user defined algorithms. The various layers have been analyzed through simulation and to date confirmed though physical observation of the working model. The conclusions about the prospective solution are made.**

I. Introduction

Everything seen in our everyday lives is seen by reflected light. The surface of virtually every material with the exception of mirrored surfaces is such that light is reflected from it in all directions diffusely and therefore, in typical circumstances, the brightness of surfaces seems to us to be about the same no matter from what direction we look at them. We are also accustomed to having bright light available from our lighting fixtures indoors, so that things can be easily seen. With enough available light, our eyes are sufficiently sensitive that diffuse reflection works well to see our way. Lighting is one of the most energy consuming industrial and household technologies. According to [1] about 19% of the electrical energy produced around the world is devoted to lighting. Therefore it is quite reasonable to utilize this emitted source as one part of the project, that of incident light. The second part refers to that of reflected light, that is, all light emanating from any source which is reflected by an object. The third part refers to ambient light, which is the combination of light reflections from various surfaces producing a uniform illumination called ambience. Available light or ambient light refers to any source of light that is not explicitly supplied by an incident source. The forth consisting of two parts being, ambient infrared radiation and stationary infrared radiation.

The total data resulting singularly from any one of the above referred emissions is negligible from a mapping perspective, however through the use of a weighted system it can be seen that valuable data may be extracted for a more complete analysis of an environment. It was also desirable from the commencement of the project to eliminate the need for the mobile robot to emit its own sources of radiation such as infrared distancing or ultrasonic range sensors in order to gauge its surroundings. Such devices may be used in some other area of its subsystems according to the requirements of the user.

We look to achieving a measuring of emitted wavelengths over a 360^{o} circumference of a mobile robot with subsequent conversion to photovoltaic measurement which can then be processed either by analogue or digital and algorithmic means.

II. The Sensor Array

The sensor array is designed with three differing types of sensor. The lower sensors as depicted in Fig.1, are near-infrared sensors with a wavelength value, λ of approximately 700nm to 1100nm and a peak sensitivity of 900nm, allowing an accurate measurement covering 400nm of the near infrared spectrum. The second row of sensors in (Fig. 1), are covering that portion of the visible spectrum, λ of around 350nm to 700nm with a spectral peak of 550nm. The top row consists of Light Emitting Diodes (LED's). The purpose to this is that the photodiodes are 'tuned', if you took away the band pass filter on a photodiode your diode would simply 'consume' all wavelengths of light until subsequent saturation, this is why they are all 'tuned' to a specific wavelength which of course allows varying degrees of receptivity both sides of their designed frequency.

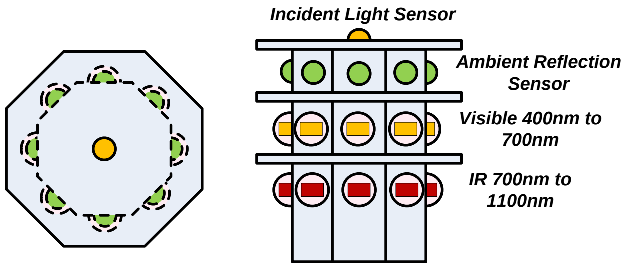

Fig.1. Sensor array configuration.

LED's however, although not specifically photodiodes and emitting much less current in reverse bias mode, offer one redeeming feature being that an LED will be receptive to wavelengths of light, less than their own wavelength and not more than their own. For example a red LED at λ = 635nm will be receptive to all wavelengths from 635nm down through the whole spectrum. The green LED I have selected is of λ=560nm and is receptive down to 430nm. This method resolves two problems. First is that the second row of photodiodes is most sensitive to λ=550nm and above. Therefore, utilizing the LED's characteristic we are able to

DOI: 10.2478/v10144-011-0021-y *2011*
Volume 29

sensitize the array sufficiently to enable a total sensitivity crossing the whole visible spectrum. The second problem solved is that 'most ambient light is at a level of mid-visible spectrum to low visible spectrum', in other words our average ambient light in our average rooms in our average homes is mostly reflected light and is in that lower range of 430nm to 570nm. One problem created is that these 560nm LED's produce an extremely low µA in reverse bias mode and require much amplification to be useful, though the use of LED's is preferable to locating photodiodes and adding appropriate colored band pass filters until obtaining the required spectral response.

The sensor array has been designed in a horizontal plane with three levels of sensors totaling 24 plus the additional Cds, (Light Dependant Resistor) above, which adjusts the overall incident light level for the sensors. Each of the three planes of sensors are arranged to cover eight sectors of a 360^o circumference. The individual sensors each have an approximate ½ Angle of 60^o giving a peripheral vision sensor of 120^o as depicted in (Fig. 2).

There is some degree of overlap of the sensors receptivity angle, a differential zone, yet 120^o is not in fact a true measure of the sensitivity range. Looking to (Fig. 3), we can see that the sensitivity angle is in fact highest at ½ Angle of 30^o with a receptivity of 0.8 to 1.

This is true of most sensors and so an overall angle of 60^o suits the purpose: $60^o * 8_{sectors} = 480 – 360^o = 120 / 8 = 15^o$, giving a differential zone of 15^o between each sensor. Overall this appears the most appropriate configuration.

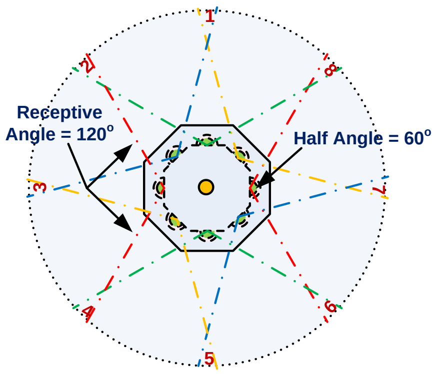

Fig.2. Sensor grid.

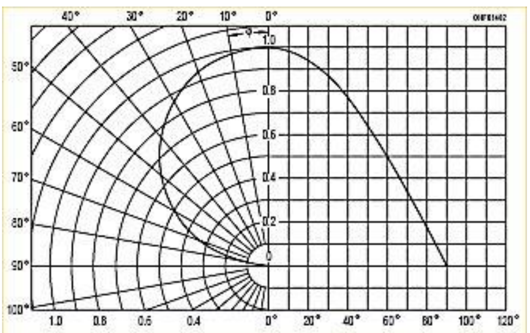

Fig.3. Directional characteristics of selected sensors.

III. Responsivity of Sensor Array

The output voltage, being a function of the amount of radiation sensed at the input is the basis for the sensor array. Therefore we are interested in the responsivity of the sensors. Electrical response depends on the response of the detector due to incident radiation across its substrate. The sensor system outlined in this paper has three basic elements. These are the sensors, amplifiers and comparators with the addition of a governing incident light detector.

Specifically attention was paid to (a) current response R_I, and (b) voltage response R_V [2], where:

c': volume specific heat (J/cm3K);
c : specific heat of material (J/gmK);
ρ : density (gm/cm3);
b : sensor thickness (µm);
GR : irradiative conductance (W/cmK);
A : detector area (cm2);
η : emissivity of the crystal;
σ : Stefan-Boltzmann constant (5.67x10-12 W/cm2K4);
T : temperature (K).

(a) <u>Current responsivity of various photovoltaic materials:</u>

R_I is the ratio of the output current flow ΔI to the input radiation power incident to detector surface Pi. The current responsivity can be calculated as [3], [4]:

$$R_I = \frac{\Delta_I}{P_I}. \quad (1)$$

Pyroelectric charge ΔQ is given by: (for infrared sensors)

$$\Delta Q = \Delta I = pA\Delta T = AP_s, \quad (2)$$

where p is the pyroelectric coefficient of material and P_S is the polarization.

Suppose that radiation power is a sinusoidal function, therefore, temperature changes of whatever detector due to irradiation flux is given by the steady-state equation as [4]:

$$\Delta T = \frac{\eta P_i}{c'bA}\frac{\tau}{\left(1+\omega^2\tau^2\right)^{1/2}}. \quad (3)$$

Substituting (2) and (3) into (1), the final expression for this current responsivity becomes (4):

$$R_I = \frac{p\eta\tau}{c'b\left(1+\omega^2\tau^2\right)^{1/2}}. \quad (4)$$

(b) <u>Voltage responsivity of various photovoltaic material:</u>

R_V is determined as a ratio of the voltage generated in the detector ΔV and radiation power incident to detector surface Pi. From this definition, we have [3], [4], [5]:

$$R_V = \frac{\Delta_V}{P_i}. \quad (5)$$

Scientific Journal of Riga Technical University
Power and Electrical Engineering
DOI: 10.2478/v10144-011-0021-y 2011
Volume 29

The generated detector voltage is given by:

$$\Delta V = \frac{\Delta Q}{C_d}, \tag{6}$$

where ΔQ = pAΔT is electric charge and *Cd* = *εrε0A/b* is detector capacitance.

When substituting (2), (3) and (5) into (6), we get the final expression for the voltage responsivity (7):

$$R_V = \frac{p\eta\tau}{c'\varepsilon_r\varepsilon_0 A\left(1+\omega^2\tau^2\right)^{1/2}}. \tag{7}$$

Graphs, indicating the wavelength dependency of the voltage responsivity for different pyroelectric materials may be located at [2].

IV. Simplified Electrical Considerations

The sensors used are in effect small flat-plate capacitors with a typical capacitance of approximately 30pF. Insulation resistance is $5\text{x}10^{12}$ Ohms. Sensors are followed by transimpedance amplifiers for current mode. Formula (8) will suffice to estimate the expected signal to be obtained from common detectors:

$$I \times \left(\frac{R}{\sqrt{1+(2\pi fRC)^2}}\right), \tag{8}$$

where:
I: can be found to be from 0.5 to 1 micro-amp per watt.
R: can be the value of the load or feedback resistor.
C: can be the sensor capacitance for voltage mode, typically 30 pF, or use stray feedback capacitance for current mode, typically 0.03pF.

V. Amplification in Photovoltaic Mode

As in (Fig. 4-a), an inverting amplifier circuit is used where the operational amplifier is connected with feedback to produce a closed loop operation. For ideal op-amps there are two very important rules to remember about inverting amplifiers, these are: "no current flows into the input terminal" and that "U1 equals U2", (in real op-amps both these rules are broken). This is because the junction of the input and feedback signal (X) is at the same potential as the positive (+) input which is at zero volts or ground then, the junction is a "Virtual Earth". Because of this virtual earth node the input resistance of the amplifier is equal to the value of the input resistor, Rin and the closed loop gain of the inverting amplifier can be set by the ratio of the two external resistors [6].

The project utilizes 24 transimpedance amplifiers as the method to convert the photodiode current to a voltage and keep the diode voltage at zero to (Fig. 4-b). It is a useful application of an inverting amplifier (Current "in", Voltage "out").

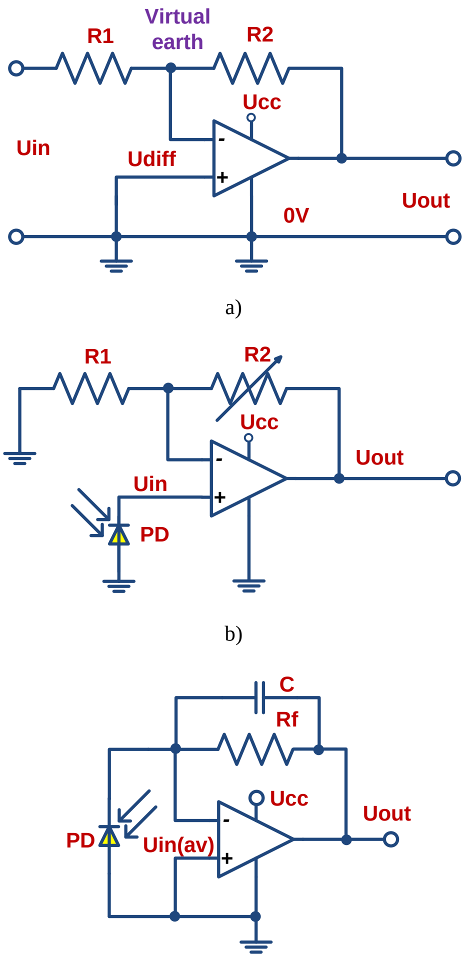

Fig.4. Circuits useful with photodiode sensors: a) inverting amplifier; b) non-inverting amplifier with photodiode and adjustable gain; c) transimpedance amplifier.

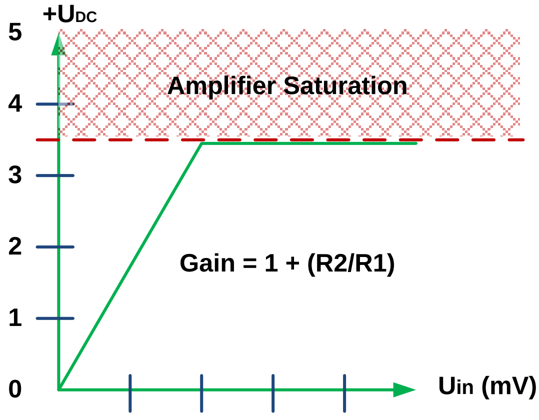

Fig.5. Transimpedance amplifier.

The output current vs. incident light can be linear over 6-9 orders of magnitude as in to (Fig. 5).When light hits the photodiode a current is generated that flows through R_F to the output (no current flows into the op-amp). The output voltage will be negative. If the diode polarity is reversed the output voltage will be positive.

Scientific Journal of Riga Technical University
Power and Electrical Engineering
DOI: 10.2478/v10144-011-0021-y 2011
Volume 29

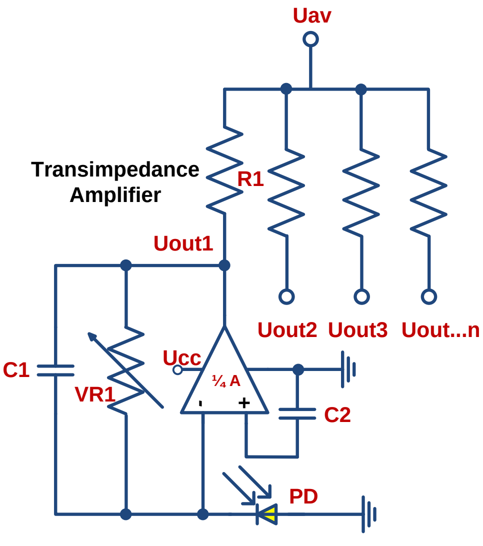

Fig.6. Passive averaging of Uout1 to Uout8.

The simple light-activated circuit shown in Fig.4-c converts a current generated by the photo-diode into a voltage.

The feedback resistor Rf sets the operating voltage point at the inverting input and controls the amount of output.

The output voltage is given as (9):

$$U_{out} = I_s \times R_f \, . \tag{9}$$

Therefore, the output voltage is proportional to the amount of input current generated by the photo-diode.

VI. Passive Averaging

The measurement of the ambient light field, 360°, of the environment is critical to the performance of the sensors used. The measure of each sensor must be controlled through 'weighting' the system to provide the 'decision making' comparators within the circuit a voltage reference, Uref .

The circuit in (Fig. 6) is commonly referred to as a passive averager. Equation (10) comes from Millman's Theorem [7], which describes the voltage produced by multiple voltage sources connected together through individual resistances. A quite simple equation however in the first stages of this project we utilize Uav to ascertain the Uref for the comparators but it may eventuate that Umax or Umin become a more useful option and in this respect and in this layer of the circuit, Millman's Equation will be extremely useful.

$$U_{av} = \frac{\frac{U_{out1}}{R_1} + \frac{U_{out2}}{R_2} + \frac{U_{out.n}}{R_n}}{\frac{1}{R_1} + \frac{1}{R_2} + \frac{1}{R_n}} \tag{10}$$

Looking at this stage for a mean average of the amplified voltages, the 8 resistors in the averager circuit are equal to each other at 1kΩ, so resulting in (11).

$$\frac{\sum_{k=1}^{n=8} a_k}{8} = U_{av} \tag{11}$$

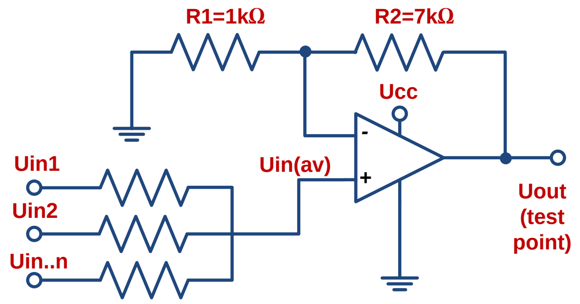

Fig.7. Non-inverting summer circuit.

VII. Non-Inverting Summer Circuit

Taking the passive averager Uav and connecting to an operational amplifier circuit with a gain of 8 we can take this averaging function and create an addition function by utilizing the non-inverting summer circuit in (Fig. 7).

The voltage divider, R1 and R2 respectively are composed of a 7kΩ / 1kΩ combination, this gives the non-inverting amplifier circuit a voltage gain of 8. By taking the Uav from the passive averager, which is the sum of Uin1 to Uin8 divided by 8, and multiplying that average by 8, we arrive at an output voltage equal to the sum of Uin1 to Uin8. With the 8 averaging resistors connected to the non-inverting input, the voltage at the inverting input is free to float to the average value of Uin1 to Uin8. With all resistor values for now equal to each other, the currents through each of the three resistors will be proportional to their respective input voltages. Those eight currents will produce at the inverting input at

Uout / 8volts and the algebraic sum of those currents through the feedback resistor will produce a voltage at Uout equal to Uin1 + Uin2 + ... Uin..n.

VIII. Incident Light Monitor

To govern the sensor array an incident light sensor on the top of the array enables accurate balancing of the numerous sensors. To achieve this we use a CdS photoconductive cell (LDR) as a component of a simple voltage divider. Most LDR's have a peak spectral wavelength of around λ=550nm as this is the approximate midway mark of the visible light spectrum.

To stabilise the LDR we use it in conjunction with a variable resistor in a voltage divider configuration as in (Fig. 8). The LDR in this case receives input from both the passive averaging circuit and the Incident light on its' Cds cell.

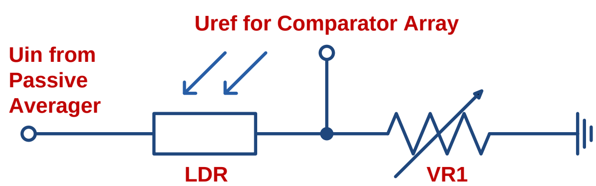

Fig.8. Adjustable potential divider.

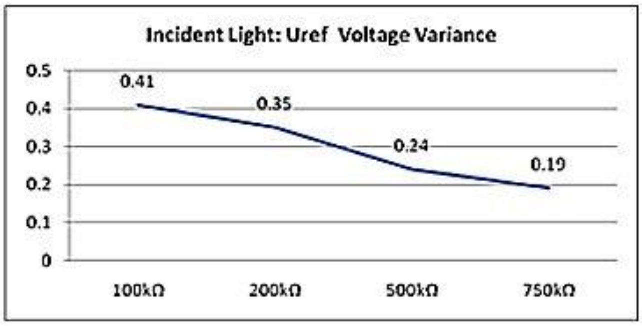

Fig.9. Reference voltage as a function of LDR

The output voltage Uref is forwarded to the comparator array in the circuit and becomes the reference voltage at their inverting inputs and is given in (12).

$$U_{ref} = \frac{VR1}{VR1 + LDR} = U_{in} \qquad (12)$$

The properties of LDR's are that with increasing light comes decreasing resistance so that in complete darkness the resistance will soar to approximately 20MΩ and more. In an average lit environment (say 10 to 100 Lux) it will be somewhere around 50 kΩ to 100kΩ, so it is easy to conclude the benefits to our system from the following. Suppose the LDR has a resistance of 75kΩ in our average environment and 200kΩ in a darker part of the environment. We want to maintain our original passive averager Uref initially so VR1 must be set approximately 10 X greater resistance than the LDR which would be let's say (470kΩ) as it is a common component value. Assuming our passive average voltage is 0.5 Uin. By equation (11) this will yield a resultant 0.43 volts.

When our mobile robot wanders into a darker area with the LDR increasing in resistance from 75kΩ to say 200kΩ the resultant yield becomes 0.35 volts. The results are quite linear as can be seen in (Fig. 9) and as a reference voltage for the comparator inputs necessarily stable.

IX. Comparator Array

The project utilizes 24 comparators as the first layer of filtering in the system. All the sensors from every sector give out some reading upon amplification. All environmental sectors from our mobile robots perspective are similar in the 360^o circumference. So that, a sensor in sector 8 may detect and have amplified a signal of 50mV and a sensor in sector 4, in the opposing direction may have detected say 30mV. In real terms there is negligible difference in those voltages. This is the purpose of the average voltage reference being referred on to the comparison system, whereby a majority of the received value will be removed as unwanted noise. In that example, the two voltages received, respectively 30mV has been amplified to 0.11V and 50mV has been amplified to 0.19V, are compared against the average and the sensor declaring 30mV is removed from the arena.

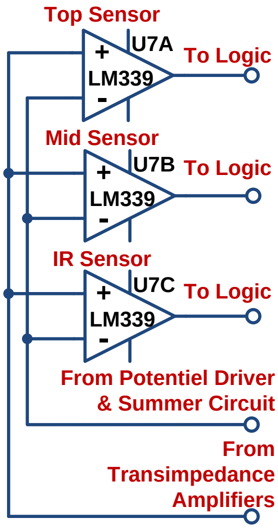

Fig.10. 1/8 of Comparator Circuit Weighting system.

For example: (0.11+0.19) / 2 = 0.15, so 0.15 becomes our U_{ref} and the 30mV sensor result is removed. Three of the necessary 24, comparators in the weighting system are denoted in (Fig. 10). The U_{ref} input at the inverting input of the comparators are connected to the LM386 which is our non-inverting summer circuit and our dedicated adjustable potential divider.

X. Logic Array

The first round of logics is accomplished in that for each sector, (remembering that each sector comprises three sensors), a Majority Adding circuit is applied comprising, three 2 input nand gates followed by one 3 input nand gate. The logic is simple enough. If any two of the inputs are high, then the output '12' in (Fig. 11) will be high. If any two are low then '12' will be low. The selection of this configuration is specific working on a three input per sector configuration. Currently, due to the weighting and testing of the system, Infrared is not as yet a priority, so has been set to logic '0' the top sensor may be high and mid sensor may be low, so effectively in this example '1' & '0' & '0' will give us a '0' logic output, so in this case is removed from the system. However another or other sectors may be at '1' & '1' & '0' which by majority makes them Logic '1'.

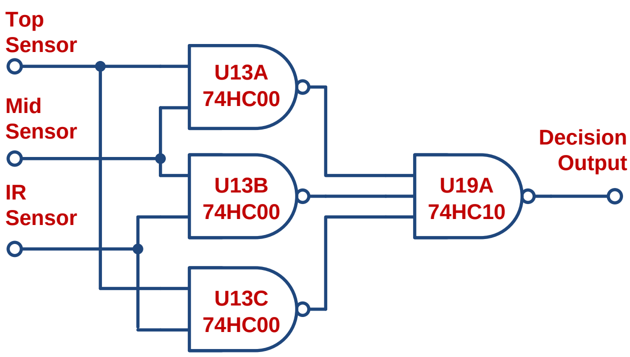

Fig.11. 1/8 of Majority Logic Circuitry.

The result is that the output is reduced from 24 sensors to 8. The remainder of the logic for the circuit resides on the second circuit which connects directly to the motor drivers.

XI. Assumptions for Weighting Sensors

Upper level sensors: These sensors have two tasks, being to determine the ambient light level in conjunction with the incident light meter to provide the weight for the other sensors and to measure that light in the level of the spectrum from midway (green) to the lower range (blue). So the preliminary assumptions are that for the upper level sensors, the brightest illumination in the environment will be the priority.

Middle level sensors: These sensors measure light over the whole visible spectrum. The mid sensors, having the whole of the visible spectrum as their source would set of course the brightest zone as priority as unlike the other sensors, have a greater ability to detect shaded areas. Shaded areas of course represent a voltaic decrease or variance in each particular sector and logically either indicate an object of low reflectivity or the entrance to a darker environment within that sector. Shaded areas indoors, generally would point to an obstacle in close proximity, therefore initial priority would be high.

Lower level sensors: Measuring the near-infrared spectrum. The IR Sensors will always detect infrared radiation as it is everywhere however we may assume that a higher level of infrared could be damaging to our mobile robot so from this perspective the lowest IR emission should be more preferable and set initially as the priority low.

XII. Conclusions

The intention of this device is to utilize existing environmental radiation, be that from the visible spectrum, (λ= 380 nm to 760 nm) or the near-infrared spectrum, (λ= 760nm to 2,5µm) and in this project, including the mid-infrared spectrum, (λ= 2,5µm to 10µm). The initial method of operation is in respect to the mobility or direction of the mobile robot. The second, to provide sufficient data to feed through logic circuitry or to microprocessor and user designated algorithm to enable environmental mapping through the use of photovoltaic means. The third is to create a generic circuit capable of providing useful data output to an assortment of control devices. The use of three sensors each with a possible six combinations, constantly and simultaneously comparing against its opposing sector has, by physical observation proved successful. Each level of components has been tested through simulation and each component layer behaves as expected, producing also some unexpected behavior which must be fully and analytically resolved in stage two of the project. For example, the addition of hardware to change between preset prioritized weights in the form of a DIP switching system appears necessary. With such a myriad of possible combinations of output the utilization of microprocessor control will be initiated in stage two also. Further, the miniaturization of the circuitry will be the subject of priority. In this initial project stage it is extremely difficult to ascertain those values which are more important to us than another. We can make certain assumptions however which over time may or may not prove correct. The system of weighting has been so designed as to enable alteration of those assumptions as the project proceeds.

References

[1] P. Waide, S. Tanishima., Light's Labor's Lost. International Energy. 9 rue de la Federation. 75739 Paris Cedex 15: IEA Publications, 2006.
[2] Analysis of MWIR Infrared Pyroelectric Detectors Parameters.
[3] G. Hyseni, N. Caka, K. Hyseni, Faculty of Electrical and Computer Engineering, Department of Electronics, Department of Automation, University of Prishtina, Republic of KOSOVA,PDF www.wseas.us/e-library/conferences/2010/Cambridge/NAICIP/NAICIP-24.pdf.
[4] P.H. Beerman, The Pyroelectric Detector of Infrared Radiation, IEEE Transaction on Electron Devices, Vol. Ed-16, No. 6. (1969).
[5] S.T. Liu, D. Long, "Pyroelectric Detectors and Materials", Proceedings of the IEEE, Vol. 66, No. 1, (1978).
[6] R. Ciupa, A. Rogalski, Performance Limitations of Photon and Thermal Infrared Detectors, Opto-Electrics. Rev.,5, no. 4, 1997.
[7] Wayne Storr. 1998 − 2010, Electronics-Tutorials.ws 'Inverting Operational Amplifiers'
[8] Tony R. Kuphaldt, „Electric Circuits" Fifth Edition, 2004 Millman's Theorem p.348.

Leslie R. Adrian received his Bachelor's (February 2009) and Master's Diploma in (February 2011) at Riga Technical University, within the Faculty of Electronics and Telecommunications (FET) and the Faculty of Power and Electrical Engineering, Department of Power Electronics and Electrical Technologies (EEF). Both theses focused on the research and development of Robotics Mobility with particular focus on Obstacle Avoidance in Robotics. Another field of research includes magnetic in power generation. Being a latecomer to Academic Studies, Leslies' work experience ranging 30 years in areas as diverse as Construction, Robotics Manufacturing, Electronics Component Distribution and as Telecommunications Server Administrator for Onelink Inc., Canada. From an Entrepreneurial perspective, Leslie has operated businesses in both Telecommunications and Electronics since 1994, with his present focus toward a European wide Robotics competition and education system. He is currently is a Doctoral Student in the Department of Power Electronics and Electrical Technologies and Lecturer of Robotics and associated studies at RTU.